Automated Robotic Needle Puncture for Percutaneous Dilatational Tracheostomy

Automated Robotic Needle Puncture for Percutaneous Dilatational Tracheostomy

Yuan Tang, Brendan McGrath, Andrew Weightman and Bruno V. Adorno

I. Introduction

Percutaneous Dilatational Tracheostomy (PDT) is routinely performed on patients who require prolonged mechanical ventilation [1]. Without the direct visualization of the trachea, the position of the PDT needle puncture is determined by palpating the patient's neck and operators' skills, resulting in large position and angular errors and associated damage caused by the needle tip [2]. The allowable puncture precision in current clinical practice is $\pm 30^\circ$ of midline deviation as long as the puncture position is close to the midline plane [3], which requires a long learning process for operators to achieve such precision every time.

Robotic technologies have been widely adopted in various minimally-invasive surgeries (MISs), demonstrating the potential to replace some manual procedures. A few prototypes were developed to perform PDT but none of them provide guidance for PDT puncture or automate the insertion process [4], [5]. Robotic systems that provide guidance using sensors and automate the needle puncture will not only achieve high precision but also release the operator's action from this step, decreasing the procedure complexity and easing clinical training. To achieve precise incision and prevent any damage caused by the robots, we use constrained controllers based on Vector-Field Inequalities (VFIs) [6]. In this framework, the dynamics between obstacles in the workspace and the robot is given by differential inequalities in a constrained optimization problem, being suitable to generate safe motions during the insertion procedure.

This research aims to adopt a robotic system that replaces the manual needle puncture and automates the process to improve puncture precision and ease the PDT training. Measuring the direction of the midline and the destination position between tracheal rings manually using electromagnetic sensors, the robot manipulator is guided using the pose information and VFI-based constrained control laws to automatically complete the puncture without colliding with the patient's body or accidentally hitting nearby tissues.

II. System Overview and Problem Formulation

Puncture procedure is divided into two steps. During the first step, the end-effector moves to the start position to align with the midline without colliding with the patient's body. During the second step, the robot advances the needle along the midline until its tip reaches the puncture destination point.

We use a constrained control law to generate the velocity control inputs $\boldsymbol{u} \triangleq \dot{\boldsymbol{q}}$. The desired task vector for the PDT puncture is given by $\boldsymbol{x}_d \in \mathbb{R}^m$ and $\dot{\boldsymbol{x}}_d$ is a feedforward term. The task error is given by $\tilde{\boldsymbol{x}} \triangleq \boldsymbol{x} - \boldsymbol{x}_d$, where $\boldsymbol{x}$ is the task vector, usually measured externally or estimated using forward kinematics. The control input $\boldsymbol{u}$ is given by

$$\begin{aligned} \boldsymbol{u} \in \operatorname{argmin} \quad & \left\| \boldsymbol{J}\dot{\boldsymbol{q}} + \eta\tilde{\boldsymbol{x}} - \dot{\boldsymbol{x}}_d \right\|_2^2 + \lambda^2 \left\| \dot{\boldsymbol{q}} \right\|_2^2 \\ \text{subject to} \quad & \boldsymbol{W}(\boldsymbol{q})\dot{\boldsymbol{q}} \preceq \boldsymbol{w}(\boldsymbol{q}), \end{aligned} \tag{1}$$

where $\boldsymbol{J} \in \mathbb{R}^{m \times n}$ is the task Jacobian for an n-DOF robot and an m-DOF task, and $\eta \in (0, \infty)$ is a proportional gain determining the convergence rate and $\lambda \in \mathbb{R}$ is the damping factor. The ℓ (scalar) linear constraints in the control inputs are represented by $\boldsymbol{W} \in \mathbb{R}^{\ell \times n}$and $\boldsymbol{w} \in \mathbb{R}^{\ell}$.

The VFIs consist of differential inequalities used to prevent collisions between the robot and geometrical primitives. A differentiable signed distance $d\left(\boldsymbol{q}\left(t\right)\right) \in \mathbb{R}$ between two collidable entities is defined, such that $\dot{d}\left(\boldsymbol{q}\left(t\right)\right) = \boldsymbol{J}_d\left(\boldsymbol{q}\right)\dot{\boldsymbol{q}}$, with $\boldsymbol{J}_d \triangleq \partial d(\boldsymbol{q})/\partial \boldsymbol{q}$ being the distance Jacobian. Then, given a constant safe distance $d_s \in [0, \infty)$ anda signed error distance $\tilde{d}(t) \triangleq d(t) - d_s$, enforcing the inequality

$$\dot{\tilde{d}}(t) \geqslant -\eta_d \tilde{d}(t) \iff -\boldsymbol{J}_d\dot{\boldsymbol{q}} \leqslant \eta_d \tilde{d}(t) \tag{2}$$

ensures that $\tilde{d}(t) \geq \tilde{d}(0)e^{-\eta_d t}$ [6]. Therefore, if $d(0) \geq d_s$, then $d(t) \geq d_s$ for all $t > 0$. An analogous reasoning applies when the inequality is reversed. If the goal is ensure $d(t) \leq d_s$, it suffices to enforce

$$\dot{\tilde{d}}(t) \leq -\eta_d \tilde{d}(t) \iff \boldsymbol{J}_d\dot{\boldsymbol{q}} \leqslant -\eta_d \tilde{d}(t). \tag{3}$$

a) First step: In the first step, the robot moves the needle tip to the puncture start location with the z-axis aligned with the puncture direction (midline) and positioned above the target puncture position with distance d_f along the midline (see Fig. 1). To avoid any part of the robot arm hitting the patient's body, we define a cylinder with a radius d_c to cover the patient's body. While moving the robot end-effector to the puncture start position, any point on robot links should not enter the restricted cylinder.

The desired task vector in (1) is given by $\boldsymbol{x}_d \triangleq \operatorname{vec}_8\left(\underline{\boldsymbol{x}}_p\underline{\boldsymbol{x}}_1\right)$, with $\underline{\boldsymbol{x}}_p$ being the unit dual quaternion representing the rigid motion from the global frame to a frame located at the insertion point, with the z-axis pointing outward, and $\underline{\boldsymbol{x}}_1 = (\boldsymbol{r}_1 + \frac{1}{2}\varepsilon\boldsymbol{p}_1\boldsymbol{r}_1)$, with $\boldsymbol{p}_1 = d_f\hat{k}$ and $\boldsymbol{r}_1 = \hat{\imath}$ (i.e., $\boldsymbol{r}_1$ is a rotation of $\pi\,\mathrm{rad}$ around the x-axis). The vec_8 operator

Y. Tang, A. Weightman and B. V. Adorno are with the Manchester Centre for Robotics and AI, University of Manchester, Manchester, UK (yuan.tang@manchester.ac.uk, andrew.weightman@manchester.ac.uk, bruno.adorno@manchester.ac.uk)

B. McGrath is with Manchester University NHS Foundation Trust, Manchester, UK (brendan.mcgrath@manchester.ac.uk)

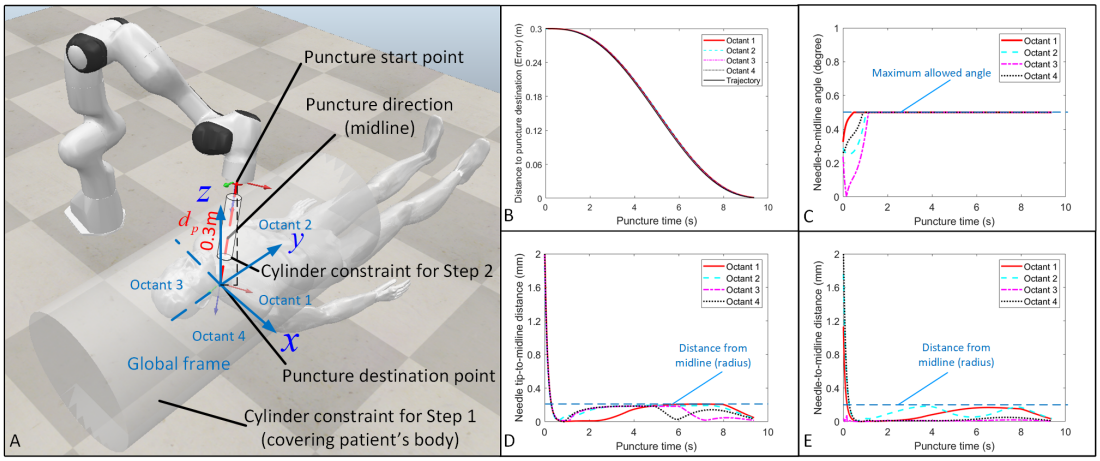

Fig. 1. (A) Simulation setup. Midline vectors were randomly selected from four octants to simulate different patient anatomy. (B) Time response of the distance between the needle tip to the puncture destination in Step 2. (C) Time response of the needle-to-midline (line-to-line) angle in Step 2. (D) Time response of the needle tip-to-midline (point-to-line) distance in Step 2. (E) Time response of the needle-to-midline (line-to-line) distance in Step 2.

maps the eight dual quaternion coefficients to a vector. The task vector is given by $\boldsymbol{x} = \mathrm{vec}_8\, \underline{\boldsymbol{x}}$, with $\underline{\boldsymbol{x}}$ being the dual quaternion representing the end-effector pose [7]. Because the desired set-point is constant, $\dot{\boldsymbol{x}}_d = \boldsymbol{0}$.

b) Second step: During the second step, two new primitives are defined to restrict the needle tip motion to inside a cylinder with small radius d_r around the puncture midline insertion, and to avoid rotating it outside a maximum allowable angle θ_p.

In this step, the needle tip position is controlled instead of its pose to release DOFs. Therefore, the task vector in (1) becomes $\boldsymbol{x} \triangleq \mathrm{vec}_3\, \boldsymbol{p}$, where $\boldsymbol{p} \in \mathbb{H}_p$ is the pure quaternion describing the needle position. The desired time-varying task vector is given by $\boldsymbol{x}_d(t) = \mathrm{vec}_3\, \boldsymbol{p}_d(t)$, where $\boldsymbol{p}_d(t) \in \mathbb{H}_p$ is generated using a quintic polynomial to ensure we can define both start and end velocities and accelerations for the needle tip [8]. The vec_3 operator maps the three coefficients of a pure quaternion to a vector in $\mathbb{R}^3$. The feedforward term is given by $\dot{\boldsymbol{x}}_d(t) = \mathrm{vec}_3\, \dot{\boldsymbol{p}}_d(t)$.

c) Constraints: The definition of constraints is done by using elements of the dual quaternion algebra [6]. For instance, to ensure that a given point $\boldsymbol{p}_r \in \mathbb{H}_p$ in the robot is outside the cylinder enclosing the patient, we consider the patient's cylinder's midline given by a Plücker line, $\underline{\boldsymbol{l}}_p = \boldsymbol{l}_p + \varepsilon \boldsymbol{p}_p \times \boldsymbol{l}_p$, with $\boldsymbol{l}_p \in \mathbb{H}_p$ being the line direction and $\boldsymbol{p}_p \in \mathbb{H}_p$ being an arbitrary point in the midline. Then, it suffices to find the (squared) distance between $\boldsymbol{p}_r$ and $\underline{\boldsymbol{l}}_p$ and its corresponding Jacobian, to define an inequality such as (2). An analogous reasoning is done to maintain any desired point inside the guiding cylinder described in Section II-0b, but an inequality such as (3) is used instead [6].

Finally, to constrain the needle tip orientation in the second step, we constrain the angle between the needle tip and the puncture guideline by using a conic constraint that is also transformed into an inequality such as (3) [9].

d) Simulation: Simulations were conducted using CoppeliaSim (Coppelia Robotics, Ltd., Switzerland) to evaluate the precision of the robotic puncture. The puncture start point is defined along the midline with a 30 cm distance from the destination. Midline vectors were randomly generated from the four octants in the global frame. The trajectory was generated using designated puncture duration $T = 10\,\mathrm{s}$ with initial and final velocities and accelerations equal to zero. Fig. II(b-e) show the time response for different aspects of the puncture procedure. We define the maximum allowed tip angle as $\theta_p = 0.5^\circ$ and the radius of the cylinder around the guiding midline as $d_r = 0.2\,\mathrm{mm}$.

III. Conclusion and Future Work

The constrained control using VFIs to ensure safe robotic tracheostomy has been verified in simulation. Future work will focus on replicating the results obtained in simulation on a real robot operating on a mannequin.

References

[1] C. G. Durbin, "Tracheostomy: why, when, and how?" *Respiratory care*, vol. 55, no. 8, pp. 1056–1068, 2010.

[2] G. Servillo and P. Pelosi, *Percutaneous tracheostomy in critically ill patients*. Springer, 2015.

[3] M. Rudas, "The role of ultrasound in percutaneous dilatational tracheostomy," *Australasian Journal of Ultrasound in Medicine*, vol. 15, no. 4, pp. 143–148, 2012.

[4] M. Botyrius, Q. Liu, C. M. Lim, and H. Ren, "Design conceptualization of a flexible robotic drill system for minimally invasive tracheostomy," in *2018 IEEE International Conference on Real-time Computing and Robotics (RCAR)*. IEEE, 2018, pp. 584–588.

[5] X. Xiao, H. Poon, C. M. Lim, M. Q.-H. Meng, and H. Ren, "Pilot study of trans-oral robotic-assisted needle direct tracheostomy puncture in patients requiring prolonged mechanical ventilation," *Frontiers in Robotics and AI*, vol. 7, p. 575445, 2020.

[6] M. M. Marinho, B. V. Adorno, K. Harada, and M. Mitsuishi, "Dynamic active constraints for surgical robots using vector-field inequalities," *IEEE Transactions on Robotics*, vol. 35, no. 5, pp. 1166–1185, 2019.

[7] B. V. Adorno, "Robot kinematic modeling and control based on dual quaternion algebra—part i: Fundamentals." 2017.

[8] M. W. Spong, S. Hutchinson, and M. Vidyasagar, *Robot modeling and control*. John Wiley & Sons, 2020.

[9] J. J. Quiroz-Omaña and B. V. Adorno, "Whole-body control with (self) collision avoidance using vector field inequalities," *IEEE Robotics and Automation Letters*, vol. 4, no. 4, pp. 4048–4053, 2019.